

that the terminal and bridging positions are clearly distinguished for **2**, **3**, and **4**. The para position is clearly identified on the basis of intensity ratio and also through the use of the complex $\text{Co}[\text{OC}(\text{4-MeC}_6\text{H}_2)_3]_2(\text{THF})_2$ (**5**), which dissociated THF in toluene to yield $[\text{Co}[\text{OC}(\text{4-MeC}_6\text{H}_{11})_3]_2]_2$ (**6**). More ambiguous are the assignments of the two most shifted and broadened peaks to the ortho hydrogens, leaving the remaining two peaks to be assigned to the meta hydrogen positions. Similar arguments have been used to assign resonances in phenyl-containing ligands of iron sulfur clusters¹⁸ and porphyrins¹⁹ before unambiguous assignments were made by using substituted phenyls.²⁰ We have assigned the downfield and upfield resonances of **2**, **3**, and **6** to the terminal and bridging groups, respectively. The addition of pyridine-*d*₅ to **5** also lends support to these assignments since only downfield Ph resonances were observed for the complex $\text{Co}[\text{OC}(\text{4-MeC}_6\text{H}_4)_3]_2(\text{py-}d_5)_2$. These assignments are also based on comparisons with terminal and bridging substituents in other transition-metal paramagnetic systems.²¹

Irrespective of the assignments in this work, it is possible to estimate an energy barrier for the dynamic ¹H NMR process seen when solutions of **2** or **6** are heated. No coalescence was observed in the THF-coordinated **3** due to irreversible changes in the

spectrum on heating. Figure 5 shows the changes in the spectrum of **2** when the compound is heated to 80 °C in C₇D₈. Free energies of activation were estimated by using an approximate formula²² based on determinations of coalescence temperature. For **2** the signals for the para hydrogens coalesce at 40 °C, affording a ΔG^\ddagger value of 57.2 kJ mol⁻¹. For the meta hydrogens, which coalesce at 75 °C, a ΔG^\ddagger value of 57.3 kJ mol⁻¹ was calculated; for **6**, very similar values of 58.7 and 56.3 kJ mol⁻¹ were obtained. Evidence for an intramolecular dynamic process comes from experiments similar to those used by Bradley et al. in their study of $[\text{Ta}(\text{OMe})_5]_2$. The addition of free ligand to either **2** or **5** in C₇D₈ solution followed by heating to coalescence showed no evidence of exchange.

Although the above studies do not establish the mechanism for intramolecular exchange, they do show that the complexes are substantially dimeric in solution at room temperature. Further studies on the dynamic ¹H NMR of various dimeric alkoxides and amides are in progress.

Acknowledgment. We thank the National Science Foundation (Grant No. CHE-811-6355) and the A. P. Sloan Foundation for financial support.

Supplementary Material Available: For the four structure determinations, full tables of bond distances and angles, anisotropic thermal parameters, and hydrogen coordinates and figures illustrating the core atoms of **1** and the ¹H NMR spectra of **2**, **3**, **4**, and **6** in C₆D₆ (26 pages); calculated and observed structure factor tables (139 pages). Ordering information is given on any current masthead page.

- (18) Kanatzidis, M. G.; Baeniziger, N. C.; Coucovanis, D.; Simopoulos, A.; Kostikas, A. *J. Am. Chem. Soc.* **1984**, *106*, 4500.
 (19) Chang, R.; Lechoslaw, L.; Balch, A. L. *Inorg. Chem.* **1982**, *21*, 2412.
 (20) Hagen, K. S.; Reynolds, J. G.; Holm, R. H. *J. Am. Chem. Soc.* **1981**, *103*, 4054.
 (21) Wolff, T. E.; Power, P. P.; Frankel, R. B.; Holm, R. H. *J. Am. Chem. Soc.* **1980**, *102*, 4694. Christou, G.; Garner, C. D.; Mabbs, F. E.; King, T. J. *J. Chem. Soc., Chem. Commun.* **1978**, 740.

- (22) Kost, D.; Carlson, E. H.; Raban, M. *J. Chem. Soc. D* **1971**, 656.
 (23) Bradley, D. C.; Holloway, C. E. *J. Chem. Soc. A* **1968**, 219.

Contribution from the Department of Chemistry,
 The University of Texas at Austin, Austin, Texas 78712

Facile Cleavage of a Phosphido Bridge with H₂. Synthesis, Structures, and Reactivities of the Heterobimetallic Complexes (MeCp)Mn(CO)₂(μ-*t*-Bu₂P)M(COD) (M = Rh, Ir; MeCp = η⁵-C₅H₄Me; COD = 1,5-Cyclooctadiene)

Atta M. Arif, Don J. Chandler, and Richard A. Jones*

Received June 11, 1986

Reaction of (MeCp)Mn(CO)₂(*t*-Bu₂PLi), generated in situ from (MeCp)Mn(CO)₂(*t*-Bu₂PH) and *n*-BuLi, with [M(COD)Cl]₂ in THF gives the dark red heterobimetallic di-*tert*-butylphosphido bridged complexes (MeCp)Mn(CO)₂(μ-*t*-Bu₂P)M(COD) [MeCp = η⁵-C₅H₄Me; COD = 1,5-cyclooctadiene; M = Rh (**1**) (89%), Ir (**2**) (82%)]. **1** and **2** have been characterized spectroscopically (IR; ¹H, ³¹P NMR) and their structures determined by X-ray crystallography. The complexes are isostructural. The molecular structures consist of a di-*tert*-butyl phosphido (*t*-Bu₂P) unit bridging a Mn-M single bond [**1**, Mn-Rh = 2.708 (2) Å; **2**, Mn-Ir = 2.637 (4) Å]. The COD ligand is bonded to give a roughly planar geometry to Rh (**1**) or Ir (**2**). The geometry at Mn in both complexes is essentially that of a three-legged piano stool (ignoring the metal-metal bond). Neither **1** nor **2** reacts with diazomethane (CH₂N₂) at room temperature in diethyl ether. Both **1** and **2** react with CO (50 psi) and excess PMe₃ although the only isolable compound in both cases is (MeCp)Mn(CO)₂(*t*-Bu₂PH). **1** does not react with H₂ (50 psi), while **2** gives (MeCp)Mn(CO)₂(*t*-Bu₂PH). Crystal data for **1**: C₂₄H₃₇MnO₂PRh, *M*_r 546.38, monoclinic, *P*₂₁/*n* (No. 1014), *a* = 17.740 (4) Å, *b* = 14.808 (3) Å, *c* = 9.051 (1) Å, β = 93.125 (2)°, *V* = 2374.2 (5) Å³, *D*_c = 1.528 g cm⁻³, *Z* = 4, λ(Mo Kα) = 0.71073 Å (graphite monochromator), μ(Mo Kα) = 12.785 cm⁻¹. Methods: MULTAN, difference Fourier, full-matrix least squares. Refinement of 2578 reflections (*I* > 3σ(*I*)) out of 3713 unique observed reflections (3° < 2θ < 48°) gives *R* and *R*_w values of 0.0495 and 0.0581, respectively. Data/parameter ratio = 9.840. Hydrogen atoms were not located. Crystal data for **2**: C₂₄H₃₇IrMnO₂P, *M*_r 635.65, monoclinic, *P*₂₁/*n* (No. 1014), *a* = 17.719 (3) Å, *b* = 14.793 (3) Å, *c* = 9.047 (2) Å, β = 93.113 (2)°, *V* = 2367.9 (5) Å³, *D*_c = 1.775 g cm⁻³, *Z* = 4, λ(Mo Kα) = 0.71073 Å (graphite monochromator), μ(Mo Kα) = 61.892 cm⁻¹. Methods: MULTAN, difference Fourier, full-matrix least squares. Refinement of 2455 reflections (*I* > 3σ(*I*)), out of 2937 unique observed reflections (2° < 2θ < 50°), gives *R* and *R*_w values of 0.0688 and 0.0760, respectively. Data/parameter ratio = 9.742. Hydrogen atoms were not located.

Introduction

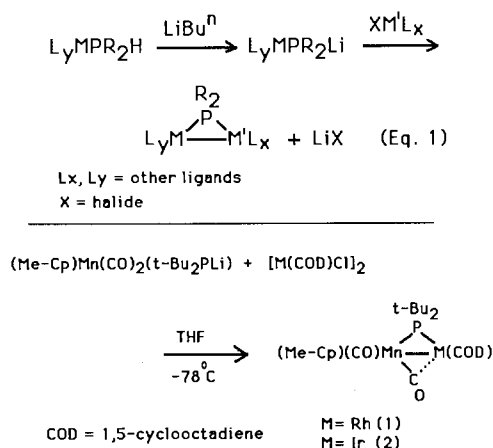
As part of a general study of heterobimetallic complexes bearing bulky phosphido (R₂P⁻) ligands, we have recently described a number of mixed-metal complexes of Cr-Rh, Cr-Ni, Cr-Co, and Fe-Ni.^{1,2} The synthesis of these complexes was accomplished

via salt elimination from the reaction of a coordinated lithiated phosphine with a metal-halide moiety (Scheme I). We report here the syntheses, X-ray structures, and preliminary chemical reactivities of two new heterobimetallic complexes; (MeC₅H₄)-Mn(CO)₂(μ-*t*-Bu₂P)M(COD) (M = Rh (**1**), Ir (**2**); COD = 1,5-cyclooctadiene). There are relatively few heterobimetallic

(1) Jones, R. A.; Lasch, J. G.; Norman, N. C.; Stuart, A. L.; Wright, T. C.; Whittlesey, B. R. *Organometallics* **1984**, *3*, 114.

(2) Chandler, D. J.; Jones, R. A.; Stuart, A. L.; Wright, T. C. *Organometallics* **1984**, *3*, 1830.

Scheme I



Mn–Rh or Mn–Ir species, examples being $(\text{CO})_4\text{Mn}(\mu\text{-Ph}_2\text{P})\text{M}(\text{CO})(\eta^5\text{-C}_5\text{H}_5)$ (M = Rh, Ir)³ and $[\text{MnRh}(\mu\text{-CO})_2(\text{CO})_2(\eta\text{-C}_5\text{H}_5)(\eta\text{-C}_5\text{Me}_5)]$.⁴

The synthesis of **1** and **2** permits a comparison of the reactivities of the Mn–Rh and Mn–Ir phosphido-bridged systems. It is interesting to note that while **1** does not react with H₂ (50 psi, 25 °C), the phosphido bridge in **2** is cleaved rapidly under similar conditions to give $(\text{MeCp})\text{Mn}(\text{CO})_2(\text{t-Bu}_2\text{PH})$ in high yield.

Results and Discussion

The reaction of the lithiated phosphine complex $(\text{MeCp})\text{Mn}(\text{CO})_2(\text{t-Bu}_2\text{PLi})$, generated in situ, with $[\text{M}(\text{COD})\text{Cl}]_2$ (M = Rh, Ir) in THF at –78 °C gives dark red solutions from which dark red crystalline $(\text{MeCp})\text{Mn}(\text{CO})_2(\mu\text{-t-Bu}_2\text{P})\text{M}(\text{COD})$ (M = Rh, **1**), Ir (**2**) can be isolated in good yields (>80%) (Scheme I). The complexes are hexane soluble and air stable for short periods although they decompose rapidly in solution when exposed to the atmosphere.

The IR spectra of both complexes show bands assignable to both terminal ($\nu_{\text{CO}} = 1935 \text{ w}, 1870 \text{ s (1)}, 1930 \text{ s}, 1860 \text{ s (2)} \text{ cm}^{-1}$) and semibridging CO groups ($\nu_{\text{CO}} = 1800 \text{ s (1)}, 1770 \text{ s (2)} \text{ cm}^{-1}$). However the ¹³C{¹H} NMR spectrum of **1** at room temperature and also at –80 °C (toluene-*d*₈) shows only one resonance for the CO units, indicating a fluxional molecule in solution (δ 263.13, d, ²J_{P-C} = 12.8 Hz at –80 °C). A process involving an intramolecular terminal–semibridge exchange that is rapid on the NMR time scale even at –80 °C would account for these observations. However, the presence of three ν_{CO} bands in the IR spectra of both compounds, both in solution and in the solid state, is difficult to reconcile with the fact that each molecule contains only two CO's. One possibility is that more than one isomer is present in both the solid state and in solution. If the interconversion of isomers is rapid on the NMR time scale but slow on the infrared time scale, this would account for our data. Although we currently have no other data to support this suggestion, of relevance here is the recent observation that $\text{Co}_2(\text{CO})_8$ is fluxional in the solid state leading to more complex IR data than would be expected from the solid-state structure.⁵ The ¹H NMR spectra are straightforward but not structurally informative while the ³¹P{¹H} NMR spectra show single resonances to low field that are indicative of a phosphido group bridging a metal–metal bond⁶ (³¹P{¹H} (**1**) δ 218.41, d, ¹J_{Rh-P} = 123.83 Hz; (**2**) δ 184.90, s).

Table I. Crystal Structure Parameters for $(\text{MeCp})\text{Mn}(\text{CO})_2(\mu\text{-t-Bu}_2\text{P})\text{Rh}(\text{COD})$ (**1**) and $(\text{MeCp})\text{Mn}(\text{CO})_2(\mu\text{-t-Bu}_2\text{P})\text{Ir}(\text{COD})$ (**2**)

	1	2
Description of Crystal		
color	dark red	dark red
habit	prism	prism
max cryst dimens, mm	0.35 × 0.30 × 0.20	0.25 × 0.25 × 0.20
Unit Cell		
cryst syst	monoclinic	monoclinic
space group	P2 ₁ /n (No. 1014)	P2 ₁ /n (No. 1014)
Unit Cell Parameters		
a, Å	17.740 (4)	17.719 (3)
b, Å	14.808 (3)	14.793 (3)
c, Å	9.051 (1)	9.047 (2)
β, deg	93.125 (2)	93.113 (2)
V, Å ³	2374.2 (5)	2367.9 (5)
molecules per unit cell	4	4
formula	C ₂₄ H ₃₇ MnO ₂ PRh	C ₂₄ H ₃₇ IrMnPO ₂
M _r	546.38	635.65
D _c , g cm ⁻³	1.528	1.775
μ _{calcd} , cm ⁻¹	12.785	61.892
Data Collection		
radiation (λ, Å)	Mo Kα (0.71073)	Mo Kα (0.71073)
scan technique	θ/2θ	θ/2θ
scan width	0.8 + 0.35 tan θ	0.8 + 0.35 tan θ
range of indices (hkl)	–20 to 20, 0 to 16, 0 to 10	0 to 20, 0 to 17, –10 to 10
2θ range, deg	3.00–48.00	2.00–50.00
no. of reflns measd	3713	2937
Standard Reflections		
intensity	3 $\bar{1}$ 5, 5 $\bar{1}$ 3	263, 6 $\bar{4}$ 3
orientation	473, 8 $\bar{6}$ 1	832, 752
decay of stds, %	1.72	7.5
min % transmissn	85.05	38.14
max % transmissn	99.50	99.80
av % transmissn	95.14	86.24
Agreement Factors for Averaged Reflections		
F(obsd)	0.024	0.035
intensity	0.028	0.048
Structure Determination		
no. of reflns used (I > 3σ(I))	3578	2455
no. of params varied	262	252
data/param ratio	9.840	9.742
shift to error ratio	0.045	1.621
esd of an observn of unit wt	3.9997	5.2116
R	0.0495	0.0688
R _w	0.0581	0.0760

Although the complexes are isostructural, they are remarkably dissimilar in their reactivity toward H₂. Both **1** and **2** react with excess PMe₃ and CO to give $(\text{MeCp})\text{Mn}(\text{CO})_2(\text{t-Bu}_2\text{PH})$ as the only isolable product in low yield (see Experimental Section). Extensive decomposition occurs during these reactions and speculation on the mechanism of formation of $(\text{MeCp})\text{Mn}(\text{CO})_2(\text{t-Bu}_2\text{PH})$ seems unwarranted. However, only **2** reacts with H₂ (50 psi, 25 °C) in THF to cleave the phosphido bridge, again giving $(\text{MeCp})\text{Mn}(\text{CO})_2(\text{t-Bu}_2\text{PH})$, while **1** remains unchanged under these conditions. Although the precise mechanism for this process is not known at present, the reasons for the difference in reactivity may lie in the greater stability of the Ir–H bonds formed by oxidative-addition reactions with H₂.⁷ Transfer of H from Ir to P and cleavage of the Ir–Mn and Ir–P bonds would then give $(\text{MeCp})\text{Mn}(\text{CO})_2(\text{t-Bu}_2\text{PH})$. Further speculation seems unwarranted since the fate of the Ir moiety of **2** could not be determined. No other complexes could be isolated from the

(3) Blickensderfer, J. R.; Kaesz, H. D. *J. Am. Chem. Soc.* **1975**, *97*, 2681.

(4) Aldridge, M. L.; Green, M.; Howard, J. A. K.; Pain, G. N.; Porter, S. J.; Stone, F. G. A.; Woodward, P. J. *Chem. Soc., Dalton Trans.* **1982**, 1333.

(5) Henson, B. E.; Sullivan, M. J.; Davis, R. J. *J. Am. Chem. Soc.* **1984**, *106*, 251.

(6) Downfield shifts in the δ 50–200 range in the ³¹P NMR of the Ph₂P groups bridging metal–metal bonds have been noted by several groups of workers. See for example: Garrou, P. E. *Chem. Rev.* **1981**, *81*, 229. Carty, A. J. *Adv. Chem. Ser.* **1982**, No. 196, 163. Kreter, P. E.; Meek, D. *Inorg. Chem.* **1983**, *22*, 319. Harley, A. D.; Guskey, G. J.; Geoffroy, G. L. *Organometallics* **1983**, *2*, 53. Similar downfield shifts have been noted for μ-t-Bu₂P complexes (see ref 1 and 2 and references therein).

(7) Collman, J. P.; Hegedus, L. S. *Principles and Applications of Organotransition Metal Chemistry*; University Science Books: Mill Valley, CA, 1980; Chapter 4, p 176.

Table II. Comparative Bond Lengths (Å) for **1** and **2**^a

	1	2		1	2
M-M	2.708 (2)	2.637 (4)	C(3)-C(4)	1.44 (2)	1.44 (4)
M-P	2.262 (2)	2.296 (6)	C(3)-C(7)	1.413 (15)	1.34 (4)
M-C(2)	2.399 (10)	2.28 (2)	C(4)-C(5)	1.41 (2)	1.37 (4)
M-C(9)	2.152 (9)	2.16 (3)	C(5)-C(6)	1.404 (15)	1.40 (5)
M-C(10)	2.146 (10)	2.13 (2)	C(6)-C(7)	1.43 (2)	1.45 (5)
M-C(13)	2.263 (10)	2.23 (2)	C(7)-C(8)	1.54 (2)	1.56 (4)
M-C(14)	2.271 (9)	2.23 (3)	C(9)-C(10)	1.423 (13)	1.45 (3)
Mn-P	2.293 (3)	2.278 (7)	C(9)-C(16)	1.527 (14)	1.40 (4)
Mn-C(1)	1.795 (10)	1.80 (3)	C(10)-C(11)	1.512 (15)	1.54 (4)
Mn-C(2)	1.779 (12)	1.78 (3)	C(11)-C(12)	1.54 (2)	1.51 (4)
Mn-C(3)	2.168 (10)	2.17 (3)	C(12)-C(13)	1.53 (2)	1.53 (4)
Mn-C(4)	2.148 (11)	2.17 (3)	C(13)-C(14)	1.377 (13)	1.40 (3)
Mn-C(5)	2.163 (12)	2.14 (3)	C(14)-C(15)	1.53 (2)	1.50 (5)
Mn-C(6)	2.165 (11)	2.17 (3)	C(15)-C(16)	1.549 (15)	1.55 (4)
Mn-C(7)	2.176 (10)	2.17 (3)	C(17)-C(18)	1.56 (2)	1.51 (4)
P-C(17)	1.923 (10)	1.93 (3)	C(17)-C(19)	1.552 (15)	1.51 (4)
P-C(21)	1.912 (10)	1.92 (3)	C(17)-C(20)	1.55 (2)	1.56 (4)
O(1)-C(1)	1.65 (7)	1.15 (3)	C(21)-C(22)	1.56 (2)	1.54 (4)
O(2)-C(2)	1.193 (14)	1.19 (4)	C(21)-C(23)	1.544 (14)	1.55 (4)
			C(21)-C(24)	1.552 (14)	1.50 (5)

^a Numbers in parentheses are the estimated standard deviations in the least significant digits.

Table III. Selected Comparative Bond Angles (deg) for **1** and **2**^a

	1	2		1	2		1	2
Mn-M-P	54.05 (6)	54.5 (2)	C(9)-M-C(13)	87.0 (4)	93.9 (9)	P-Mn-C(4)	110.4 (3)	91.0 (8)
Mn-M-C(2)	40.2 (3)	41.6 (8)	C(9)-M-C(14)	80.5 (4)	78 (1)	P-Mn-C(5)	91.4 (3)	109.8 (8)
Mn-M-C(9)	140.8 (3)	153.4 (7)	C(10)-M-C(13)	80.2 (4)	78.8 (9)	P-Mn-C(6)	108.8 (3)	148 (1)
Mn-M-C(10)	153.0 (3)	139.9 (6)	C(10)-M-C(14)	96.5 (4)	87 (1)	P-Mn-C(7)	147.0 (3)	145.4 (8)
Mn-M-C(13)	124.1 (3)	112.4 (6)	C(13)-M-C(14)	35.4 (4)	36.5 (9)	C(1)-Mn-C(2)	95.6 (5)	94 (1)
Mn-M-C(14)	110.3 (3)	126 (1)	M-Mn-P	53.00 (6)	55.1 (2)	C(1)-Mn-C(3)	115.8 (4)	96 (1)
P-M-C(2)	83.3 (3)	86.3 (8)	M-Mn-C(1)	65.3 (3)	65.8 (8)	M-P-Mn	72.95 (8)	70.4 (2)
P-M-C(9)	107.6 (3)	98.9 (7)	M-Mn-C(2)	60.5 (3)	58.4 (8)	M-P-C(17)	111.8 (3)	121.5 (7)
P-M-C(10)	99.0 (3)	107.3 (6)	M-Mn-C(3)	144.5 (3)	152.2 (8)	M-P-C(21)	121.6 (3)	112 (1)
P-M-C(13)	155.7 (3)	165.6 (6)	M-Mn-C(4)	141.0 (3)	145.1 (8)	Mn-P-C(17)	117.2 (3)	118.2 (8)
P-M-C(14)	163.1 (3)	153.7 (8)	M-Mn-C(5)	143.8 (3)	140.5 (9)	Mn-P-C(21)	119.6 (3)	117.0 (9)
C(2)-M-C(9)	164.9 (4)	151 (1)	M-Mn-C(6)	149.7 (3)	142 (1)	C(17)-P-C(21)	109.7 (4)	112 (1)
C(2)-M-C(10)	151.2 (4)	162 (1)	M-Mn-C(7)	150.5 (3)	151.2 (8)	M-C(2)-Mn	79.3 (4)	80.1 (9)
C(2)-M-C(13)	85.7 (4)	85 (1)	P-Mn-C(1)	94.2 (3)	95.0 (8)	M-C(2)-O(2)	119.5 (8)	124 (2)
C(2)-M-C(14)	85.8 (4)	85 (1)	P-Mn-C(2)	99.2 (4)	100.3 (9)	Mn-C(2)-O(2)	161.1 (9)	156 (2)
C(9)-M-C(10)	38.7 (4)	39.6 (9)	P-Mn-C(3)	149.4 (3)	109.5 (8)	Mn-C(1)-O(1)	168.7 (5)	166 (2)

^a Numbers in parentheses are the estimated standard deviations in the least significant digits.

reaction mixture nor identified by ¹H NMR.

X-ray Crystal Structures of 1 and 2. The complexes are isostructural and crystallize in the space group $P2_1/n$ with four molecules in the unit cell. A general view of **2** is shown in Figure 1; the view and labeling of **1** is quite similar. Crystallographic data are collected in Table I, and comparative bond lengths and angles for **1** and **2** are collected in Tables II and III, respectively. Positional parameters are given in Tables IV and V.

The overall molecular geometry consists of a di-*tert*-butylphosphido (*t*-Bu₂P) unit bridging a Mn-M single bond (M = Rh, Ir). Both complexes have a carbonyl unit (C(2)-O(2)) that occupies a semibridging position from Mn to Rh (or Ir). The geometry around the Rh (or Ir) atom, consisting of C(2), the P atom of the bridging *t*-Bu₂P unit, and the midpoints of the olefinic bonds of the COD units, is roughly square planar.⁸ The geometry at Mn in both complexes is essentially that of a three-legged piano stool (ignoring the metal-metal bond). Although formal electron-counting procedures are frequently misleading, in this case, one can consider the Mn atom to have a formal electron count of 18 and the Rh (or Ir) to have 16 with a dative Mn→Rh (or Ir) bond.

Despite their isostructural nature, there are some key structural differences in the two complexes. The Mn-Rh distance (2.708

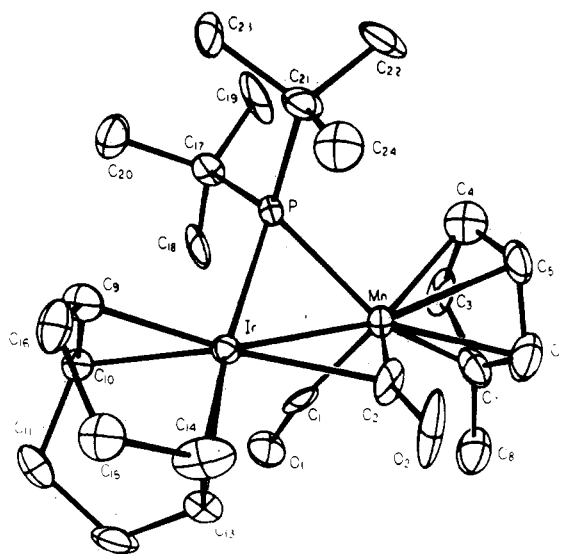


Figure 1. General view of **2** showing the atom-labeling scheme. The atom-labeling scheme for **1** is the same with Ir replaced by Rh.

(8) Deviations (Å) from the least-squares plane where C(95)) and C(135) are the midpoints of C(9)-C(10) and C(13)-C(14), respectively, are as follows: For **1**, Rh -0.066 (1), Mn 0.241 (1), P -0.265 (2), C(95) 0.240 (6), C(135) -0.150 (6), C(2) -0.804 (11); for **2**, Ir 0.054 (1), Mn -0.252 (4), P(1) 0.279 (6), C(95) -0.251 (6), C(135) 0.170 (6), C(2) -1.75 (3).

(2) Å) is significantly longer than the Mn-Ir length (2.627 (4) Å) in **2**, although both these distances fall within the limits normally found for a single metal-metal bond of this type (eg. Rh-Mn = 2.703 (2) Å in [MnRh(μ-CO)₂(CO)₂(η-C₅H₅)(η-C₅Me₅)]⁴). The longer Mn-Rh distance in **1** also results in a longer

Table IV. Positional Parameters and Their Estimated Standard Deviations for **1**

atom	x	y	z	$B, \text{\AA}^2$
Rh	0.60385 (4)	0.20207 (5)	0.17431 (8)	2.27 (1)
Mn	0.64135 (8)	0.32895 (9)	-0.0243 (2)	2.66 (3)
P	0.7189 (1)	0.2207 (2)	0.0827 (3)	2.31 (4)
O(1)	0.0254 (4)	0.2921 (5)	0.3433 (8)	4.6 (2)
O(2)	0.5600 (6)	0.4069 (5)	0.2188 (9)	7.5 (2)
C(1)	0.5716 (5)	0.2493 (7)	-0.093 (1)	3.4 (2)
C(2)	0.5924 (6)	0.3617 (7)	0.134 (1)	4.4 (3)
C(3)	0.6236 (7)	0.4677 (7)	-0.094 (1)	4.8 (3)
C(4)	0.7003 (7)	0.4552 (7)	-0.037 (1)	5.3 (3)
C(5)	0.7352 (6)	0.3916 (7)	-0.128 (1)	5.1 (3)
C(6)	0.6819 (7)	0.3634 (7)	-0.238 (1)	4.4 (2)
C(7)	0.6131 (6)	0.4108 (7)	-0.219 (1)	4.2 (2)
C(8)	0.5412 (7)	0.4088 (9)	-0.323 (1)	5.8 (3)
C(9)	0.5834 (5)	0.0592 (6)	0.190 (1)	3.1 (2)
C(10)	0.6285 (6)	0.0885 (6)	0.316 (1)	3.6 (2)
C(11)	0.6004 (7)	0.1033 (9)	0.469 (1)	5.0 (3)
C(12)	0.5232 (7)	0.1514 (9)	0.464 (1)	5.1 (3)
C(13)	0.5137 (5)	0.2207 (8)	0.339 (1)	4.1 (2)
C(14)	0.4775 (5)	0.2043 (8)	0.203 (1)	4.0 (2)
C(15)	0.4471 (6)	0.1125 (8)	0.152 (1)	4.7 (3)
C(16)	0.5004 (6)	0.0328 (7)	0.196 (1)	3.9 (2)
C(17)	0.7927 (5)	0.2598 (7)	0.233 (1)	3.6 (2)
C(18)	0.7478 (7)	0.3102 (9)	0.351 (1)	6.1 (3)
C(19)	0.8503 (6)	0.3276 (8)	0.173 (1)	5.8 (3)
C(20)	0.8358 (7)	0.1809 (8)	0.311 (1)	6.0 (3)
C(21)	0.7621 (5)	0.1308 (7)	-0.039 (1)	3.7 (2)
C(22)	0.8353 (7)	0.1654 (9)	-0.107 (1)	6.4 (3)
C(23)	0.7780 (7)	0.0418 (7)	0.046 (1)	4.7 (3)
C(24)	0.7017 (7)	0.1105 (8)	-0.165 (1)	4.5 (3)

^a B values for anisotropically refined atoms are given in the form of the isotropic equivalent thermal parameter defined as $4/3[a^2B(1,1) + b^2B(2,2) + c^2B(3,3) + ab(\cos \gamma)B(1,2) + ac(\cos \beta)B(1,3) + bc(\cos \alpha)B(2,3)]$.

Table V. Positional Parameters and Their Estimated Standard Deviations for **2**

atom	x	y	z	$B, \text{\AA}^2$
Ir	0.89528 (5)	0.29550 (6)	0.8281 (1)	2.13 (1)
Mn	0.8581 (2)	0.1731 (2)	1.0232 (4)	2.49 (7)
P	0.7774 (3)	0.2775 (4)	0.9176 (7)	2.3 (1)
O(1)	0.970 (1)	0.295 (1)	1.164 (2)	4.8 (4)
O(2)	0.946 (2)	0.096 (1)	0.792 (2)	7.6 (6)
C(1)	0.926 (1)	0.255 (2)	1.094 (3)	3.3 (5)
C(2)	0.911 (2)	0.144 (2)	0.869 (3)	4.1 (6)
C(3)	0.819 (2)	0.134 (2)	1.237 (3)	5.3 (7)
C(4)	0.765 (1)	0.105 (2)	1.122 (4)	5.5 (7) ^b
C(5)	0.802 (2)	0.045 (2)	1.035 (4)	4.8 (7)
C(6)	0.878 (2)	0.033 (2)	1.088 (4)	6.1 (9)
C(7)	0.885 (2)	0.091 (2)	1.218 (3)	4.3 (6)
C(8)	0.957 (2)	0.092 (2)	1.323 (3)	5.8 (7)
C(9)	0.872 (1)	0.409 (2)	0.682 (3)	4.0 (6)
C(10)	0.916 (1)	0.437 (2)	0.814 (3)	2.6 (4) ^b
C(11)	0.999 (1)	0.465 (2)	0.803 (3)	3.4 (5)
C(12)	1.053 (1)	0.389 (2)	0.844 (4)	4.7 (7)
C(13)	1.019 (1)	0.297 (2)	0.795 (2)	2.7 (4)
C(14)	0.981 (2)	0.278 (3)	0.659 (3)	5.4 (8)
C(15)	0.972 (2)	0.348 (2)	0.538 (4)	4.7 (6) ^b
C(16)	0.896 (2)	0.400 (2)	0.538 (3)	4.2 (7)
C(17)	0.735 (1)	0.367 (2)	1.044 (3)	3.2 (5)
C(18)	0.794 (2)	0.391 (2)	1.163 (3)	4.8 (7)
C(19)	0.663 (2)	0.333 (2)	1.109 (4)	6.7 (8)
C(20)	0.717 (2)	0.456 (2)	0.957 (4)	5.3 (8)
C(21)	0.705 (1)	0.235 (2)	0.767 (4)	4.5 (7)
C(22)	0.646 (2)	0.173 (2)	0.833 (4)	6.2 (9)
C(23)	0.663 (2)	0.315 (2)	0.688 (4)	6.6 (7)
C(24)	0.749 (2)	0.184 (3)	0.656 (4)	5 (1) ^b

^a B values for anisotropically refined atoms are given in the form of the isotropic equivalent thermal parameter defined as $4/3[a^2B(1,1) + b^2B(2,2) + c^2B(3,3) + ab(\cos \gamma)B(1,2) + ac(\cos \beta)B(1,3) + bc(\cos \alpha)B(2,3)]$. ^b B value for an isotropically refined atom.

Rh-C(2) distance for the semibridging CO unit (Rh-C(2) = 2.40 (1) Å vs. Ir-C(2) = 2.28 (2) Å). The Mn-P distance in **1** is also slightly longer than that in **2** (2.293 (3) vs. 2.278 (7) Å). In

contrast, the Rh-P bond length is shorter than the Ir-P distance (2.262 (2) vs. 2.296 (2) Å, respectively). The other metric parameters of both structures all fall within normal limits.

Experimental Section

All reactions were performed under oxygen-free nitrogen or in a vacuum. Microanalyses were by the Schwartzkopf Microanalytical Laboratory, Woodside, NY. Hexane and THF were dried over sodium and distilled from sodium benzophenone ketyl under nitrogen before use. [Rh(COD)Cl]₂⁹, [Ir(COD)Cl]₂¹⁰ and *t*-Bu₂PH¹¹ were prepared by literature methods. (MeCp)Mn(CO)₃ was obtained from Alfa Chemicals. Melting points were in sealed capillaries under nitrogen (1 atm) and are uncorrected.

Instruments: IR, Perkin-Elmer 1330; NMR, Varian EM-390 (¹H, 90 MHz), Varian FT-80 (³¹P, 32.384 MHz), Bruker WM-90 (³¹P, 36.43 MHz), and Nicolet NT-200 (¹H and ³¹P). IR spectra were run on Nujol mulls (KBr plates) or on solutions (matched KBr or CaF₂ cells). NMR spectra were recorded in C₆D₆ at ambient temperature and are referenced to Me₄Si (δ 0.0, ¹H) and 85% H₃PO₄ (aq) (δ 0.0, ³¹P).

(MeCp)Mn(CO)₂(*t*-Bu₂PH). (MeCp)Mn(CO)₃ (7.15 g, 32.8 mmol) and *t*-Bu₂PH (4.79 g, 32.8 mmol) were dissolved in hexane (100 mL) in a quartz Schlenk vessel. The solution was stirred magnetically and photolyzed (19 h) with a 550-W Hanovia mercury vapor lamp. Cooling (-20 °C) gave bright yellow needles of MeCpMn(CO)₂(*t*-Bu₂PH), which were collected and dried under vacuum. Yield: 8.8 g (80%). Mp: 80–81 °C. IR: (hexane, KBr matched cells), 1930 s, 1865 s, (cm⁻¹). ³¹P{¹H} NMR δ 115.49 (m); in the proton-coupled spectrum a doublet of multiplets is observed: ¹J_{P-H} = 319.20 Hz. ¹H NMR: δ 4.10 (d, 1 H, ¹J_{P-H} = 312 Hz, P-H), 3.95 (m, 4 H, MeC₅H₄), 1.72 (s, 3 H, MeCp), 1.30 (d, 18 H, ²J_{P-H} = 13.5 Hz, *t*-Bu₂P).

(MeCp)Mn(CO)₂(μ -*t*-Bu₂P)Rh(COD) (1). A solution of (MeCp)Mn(CO)₂(*t*-Bu₂PH) (0.41 g, 1.22 mmol) in THF (40 mL) was cooled (-78 °C) and 1 molar equiv of *n*-BuLi (hexane solution) was added. The resulting orange solution was allowed to warm to -20 °C and then added dropwise to a solution of [Rh(COD)Cl]₂ (0.30 g, 0.61 mmol) in THF (40 mL) at room temperature. The dark red solution was stirred magnetically for 2 h, volatile materials were removed under vacuum, and the remaining residue was extracted into hexane (2 × 30 mL). The resulting solution was filtered, and the filtrate was concentrated (ca. 10 mL). Cooling (-20 °C) for 10 h gave dark red crystals of **1**. They were collected and dried under vacuum. Yield: 0.59 g (89%). Mp: 134–136 °C dec. IR (Nujol mull, KBr plates): 1935 w, 1870 s, 1800 s cm⁻¹. ¹H NMR (90 MHz): δ 5.53 (br, $\Delta w_{1/2}$ = 9 Hz, 2 H COD), 4.80 (br, $\Delta w_{1/2}$ = 9 Hz, 2 H, COD), 4.65 (br, $\Delta w_{1/2}$ = 6 Hz, 2 H, C₅H₄Me), 4.30 (br, $\Delta w_{1/2}$ = 6 Hz, 2 H, C₅H₄Me), 2.25 (br m, $\Delta w_{1/2}$ = 18 Hz, 8 H, COD), 1.90 (s, 3 H, C₅H₄Me), 1.24 (d, J_{P-H} = 12 Hz, 18 H, *t*-Bu₂P). ³¹P{¹H} NMR: δ 218.41 (d, ¹J_{Rh-P} = 123.83 Hz). Anal. Calcd for C₂₄H₃₇MnO₂PRh: C, 52.76; H, 6.83. Found: C, 53.00; H, 6.71.

(MeCp)Mn(CO)₂(μ -*t*-Bu₂P)Ir(COD) (2). A procedure similar to that used for the synthesis of **1** was used. Yield: 82%. Mp: 120–122 °C. IR (hexane, KBr cells): 1930 s, 1860 s, 1770 s cm⁻¹. ¹H NMR (90 MHz): δ 4.75 (br, $\Delta w_{1/2}$ = 12 Hz, 2 H, COD), 4.48 (br, $\Delta w_{1/2}$ = 12 Hz, 2 H, COD), 4.12 (br, $\Delta w_{1/2}$ = 4 Hz, 2 H, C₅H₄Me), 4.00 (br, $\Delta w_{1/2}$ = 4 Hz, 2 H, C₅H₄Me), 2.15 (br m, $\Delta w_{1/2}$ = 18 Hz, 8 H, COD), 1.81 (s, 3 H, C₅H₄Me), 1.18 (d, J_{P-H} = 13.5 Hz, 18 H, *t*-Bu₂P). ³¹P{¹H} NMR: δ 184.9 (s). Anal. Calcd for C₂₄H₃₇IrMnO₂P: C, 45.31; H, 5.82. Found: C, 45.22; H, 5.57.

Reactions of 1 and 2 with CO, PMe₃, and H₂. CO. Carbon monoxide (1 atm) was bubbled through a THF solution of **1** or **2** for 15 min at room temperature. During this time, the color of the solutions changed from deep red to yellow. Volatile materials were then removed under vacuum, and the residue was extracted into hexane. The solutions were filtered and cooled (-20 °C) to give (MeCp)Mn(CO)₂(*t*-Bu₂PH) in very low yields. A brown intractable residue remains after the hexane extraction.

PMe₃. Excess PMe₃ was added to a THF solution of **1** or **2** at 25 °C. The solutions were stirred (magnetic follower) (48 h) during which time the color of the solutions changed from dark red to yellow. Workup similar to that used for reactions with CO (above) gave low yields of (MeCp)Mn(CO)₂(*t*-Bu₂PH) (ca. 5%).

Reaction of 1 with H₂. A THF solution of **1** was pressurized with H₂ (50 psi) and heated to 50 °C (24h). No reaction took place as evidenced by ³¹P NMR spectroscopy.

Reaction of 2 with H₂. H₂ (1 atm) was bubbled through a THF solution of **2** (5 min). During this time, the color changed from dark red

(9) Giordano, G.; Crabtree, R. H. *Inorg. Synth.* 1979, 19, 218.

(10) Herde, J. L.; Lambert, J. C.; Senoff, C. V. *Inorg. Synth.* 1974, 15, 18.

(11) Hoffman, H.; Schellenbeck, P. *Chem. Ber.* 1966, 99, 1134.

to yellow. Evaporation to dryness and extraction into hexane gave only $\text{MeCpMn}(\text{CO}_2(t\text{-Bu})\text{PH})$ (15%). An intractable residue, presumably containing unidentified Ir species, was left after the hexane extraction.

X-ray Experimental Section

General Procedures. Data were collected on an Enraf-Nonius CAD-4 diffractometer by using graphite-monochromated $\text{Mo K}\alpha$ radiation. Data were collected by the $\theta/2\theta$ scan technique at $23 \pm 2^\circ\text{C}$. Details of the standard data collection methods were similar to those outlined in ref 12. All calculations were performed on a PDP 11/44 computer using the Enraf-Nonius software package SDP PLUS.¹³

Crystals of **1** and **2** were grown from hexane solution at -20°C and mounted in thin-walled glass capillaries under nitrogen. Unit cell parameters were obtained by carefully centering 25 reflections having 2θ values between 24.0 and 26.0° for **1** and 22.0 and 24.0° for **2**. For both compounds, the monoclinic space group $P2_1/n$ (No. 1014) was uniquely determined by systematic absences ($h0l$, $h + l = 2n + 1$; $0k0$, $k = 2n + 1$; $h00$, $h = 2n + 1$; $00l$, $l = 2n + 1$). Data were collected in the $\pm h, \pm k, \pm l$ and $+h, +k, \pm l$ quadrants for **1** and **2**, respectively. Details of crystal data parameters and other relevant information are collected in Table I. For both structures, the data were corrected for Lorentz and polarization effects and also for absorption by using an empirical ψ scan method program (program EAC). For **2**, a 7.5% decay of the standard reflections occurred, and so an anisotropic decay correction was applied. The observed structure factors of equivalent reflections were averaged. Both structures were solved by direct methods (SIMPEL) followed by successive cycles of difference Fourier maps followed by least-squares refinement. A non-Poisson contribution weighting scheme with an ex-

perimental instability factor, P , was used in the final stages of refinement ($P = 0.05$ for both **1** and **2**).¹⁴ All non-hydrogen atoms were refined anisotropically for **1**. For **2** all non-hydrogen atoms except for C(4), C(10), C(15), and C(24) were refined anisotropically. Hydrogen atoms were not located in either structure.

For **1**, the maximum peak in the final difference Fourier map had a height of $0.67 \text{ e } \text{\AA}^{-3}$ and was located 0.89 \AA from C(14). For **2**, the maximum peak in the final difference Fourier was $0.855 \text{ e } \text{\AA}^{-3}$ and was 0.90 \AA from Ir. Scattering factors were taken from ref 15. Supplementary material is available.¹⁶

Acknowledgment. We thank the Robert A. Welch Foundation (Grant F-816), the National Science Foundation (Grant CHE-8517759), and the Texas Advanced Technology Research Program for support. We also thank Johnson Matthey, Inc., for generous loans of $\text{RhCl}_3 \cdot x\text{H}_2\text{O}$ and $\text{IrCl}_3 \cdot x\text{H}_2\text{O}$. R.A.J. thanks the Alfred P. Sloan Foundation for a fellowship (1985-1987).

Supplementary Material Available: Complete listings of bond angles and thermal parameters (8 pages); tables of observed and calculated structure factors (51 pages). Ordering information is given on any current masthead page.

(12) Jones, R. A.; Wright, T. C.; *Organometallics* **1983**, *2*, 1842.

(13) *SDP-PLUS*, 4th Ed.; B. A. Frenz and Associates: College Station, TX, 1981.

(14) P is used in the calculation of $\sigma(I)$ to downweight intense reflections in the least-squares refinement. The function minimized was $\sum w(|F_o| - |F_c|)^2$ where $w = 4(F_o)^2 / [\sum (F_o)^2]^2$, where $[\sum (F_o)^2]^2 = [S^2(C + R^2B) + \{P(F_o)^2\}^2] / (Lp)^2$, where S is the scan rate, C is the total integrated peak count, R is the ratio of scan time to background counting time, B is the total background count and Lp is the Lorentz-polarization factor.

(15) *International Tables for X-Ray Crystallography*; Kynoch: Birmingham, England, 1974; Vol. 4.

(16) See paragraph at end of paper regarding supplementary material.

Contribution from the Department of Chemistry, Purdue University, West Lafayette, Indiana 47907

Preparation and Spectroscopic Characterization of the Series of Mixed-Ligand Complexes $\text{Mo}_2\text{X}_n(\text{mhp})_{4-n}(\text{PR}_3)_n$ ($\text{X} = \text{Cl, Br}$; $\text{PR}_3 = \text{PMePh}_2, \text{PMe}_2\text{Ph}, \text{PEt}_3$; $\text{mhp} = \text{Anion of 2-Hydroxy-6-methylpyridine}$; $n = 1-3$)

William S. Harwood, S. Mark Kennedy, Fred E. Lytle,* Ju-sheng Qi, and Richard A. Walton*

Received October 21, 1986

The mixed-ligand complexes $\text{Mo}_2\text{X}_2(\text{mhp})_2(\text{PR}_3)_2$ ($\text{X} = \text{Cl, Br}$; $\text{mhp} = \text{monoanion of 2-hydroxy-6-methylpyridine}$; $\text{PR}_3 = \text{PEt}_3, \text{PMe}_2\text{Ph}, \text{PMePh}_2$) have been prepared through the reactions of $\text{Mo}_2\text{X}_4(\text{PR}_3)_4$ with Hmhp in toluene and ligand redistribution reactions on admixing equimolar amounts of $\text{Mo}_2\text{X}_4(\text{PR}_3)_4$ and $\text{Mo}_2(\text{mhp})_4$ in toluene. Similar procedures can be used to prepare the chloride complexes $\text{Mo}_2\text{Cl}_2(\text{mhp})(\text{PR}_3)_3$ and $\text{Mo}_2\text{Cl}(\text{mhp})_3(\text{PR}_3)$. The 2,4-dimethyl-6-hydroxypyrimidine analogues $\text{Mo}_2\text{X}_2(\text{dmhp})_2(\text{PEt}_3)_2$ ($\text{X} = \text{Cl, Br}$) were prepared from the reactions between $\text{Mo}_2\text{X}_4(\text{PEt}_3)_4$ and Hdmhp. The complexes $\text{Mo}_2\text{X}_2(\text{mhp})_2(\text{PR}_3)_2$ and $\text{Mo}_2\text{X}_2(\text{dmhp})_2(\text{PEt}_3)_2$ possess very similar ^{31}P NMR and electronic absorption spectral properties and display similar cyclic voltammograms, thereby indicating their close structural relationship to the structurally characterized derivative *cis*- $\text{Mo}_2\text{Cl}_2(\text{mhp})_2(\text{PEt}_3)_2$. The $^{31}\text{P}\{^1\text{H}\}$ NMR spectra of $\text{Mo}_2\text{X}_2(\text{mhp})(\text{PR}_3)_3$ show a doublet and a triplet ($J(\text{P-P}) \approx 14 \text{ Hz}$; intensity ratio doublet:triplet = 2:1), which accords with these complexes possessing a structure in which a pair of trans PR_3 ligands are mutually *cis* to the O atom of the mhp bridge, while the other phosphine is *trans* to the N atom of the bridging ligand at the other Mo atom. Electrochemical measurements on $\text{Mo}_2\text{X}_n(\text{mhp})_{4-n}(\text{PR}_3)_n$ show the presence of a reversible oxidation ($E_{1/2}$ between $+0.55$ and $+0.26 \text{ V}$ vs. Ag/AgCl). The $E_{1/2}$ values shift to a more negative potential as the number of mhp ligands increases. The species $\text{Mo}_2\text{X}_2(\text{mhp})_2(\text{PR}_3)_2$ exhibit an interesting case of bimodal luminescence. The emission spectra show bands at ca. 600 and ca. 400 nm, the intensities of which are reciprocally related. The intensity ratio $I(400 \text{ nm})/I(600 \text{ nm})$ increases with an increase in solvent viscosity. Models are proposed that can explain these luminescence properties.

Introduction

There are a variety of quadruply bonded dinuclear complexes that either contain no ligand bridges or have the metal atoms bridged by four monoanionic ligands.¹ Fewer complexes have been synthesized in which there are an intermediate number of anionic bridging ligands. One early example is the bis(carboxylate)-bridged compound $\text{Mo}_2\text{Br}_2(\text{O}_2\text{CPh})_2(\text{P-}n\text{-Bu})_2$,² in which the carboxylate bridges are disposed in a *trans* arrangement with

respect to one another.³ Subsequently, a variety of other dimolybdenum(II) complexes have been characterized in which a similar *trans* disposition of carboxylate groups is present.⁴ However, the alternative *cis* arrangement of carboxylate ligands

(1) Cotton, F. A.; Walton, R. A. *Multiple Bonds Between Metal Atoms*; Wiley: New York, 1982; and references therein.

(2) San Filippo, J., Jr.; Sniadoch, H. J. *Inorg. Chem.* **1976**, *15*, 2209.

(3) Potenza, J. A.; Johnson, R. J.; San Filippo, J., Jr. *Inorg. Chem.* **1976**, *15*, 2215.

(4) (a) Hursthouse, M. B.; Abdul Malik, K. M. *Acta Crystallogr., Sect. B: Struct. Crystallogr. Cryst. Chem.* **1979**, *B35*, 2709. (b) Mainz, V. V.; Andersen, R. A. *Inorg. Chem.* **1980**, *19*, 2165. (c) Green, M. L. H.; Parkin, G.; Bashkin, J.; Fail, J.; Prout, K. *J. Chem. Soc., Dalton Trans.* **1982**, 2519. (d) Girolami, G. S.; Mainz, V. V.; Andersen, R. A. *J. Am. Chem. Soc.* **1982**, *104*, 2041.